ACCOUNTS of chemical research

Article

Cite This: Acc. Chem. Res. 2018, 51, 2880−2887

pubs.acs.org/accounts

Toward Rationally Designing Surface Structures of Micro- and Nanocrystallites: Role of Supersaturation

Jiawei Zhang,[†] Huiqi Li,[†] Qin Kuang,*[,†] and Zhaoxiong Xie*[,†,‡]

[†]State Key Laboratory of Physical Chemistry of Solid Surfaces, Collaborative Innovation Center of Chemistry for Energy Materials, College of Chemistry and Chemical Engineering, Xiamen University, Xiamen 361005, China

[‡]Pen-Tung Sah Institute of Micro-Nano Science and Technology, Xiamen University, Xiamen 361005, China

CONSPECTUS: Tailoring the surface structures of nanocrystals is an exciting research area on account of appealing surface-dependent properties in various applications. Although significant progress has been made in recent years, current synthetic approaches are mainly dependent upon trial and error because of the ambiguous roles of various influencing factors in complicated environments. Therefore, a general theory for predicting and guiding the rationally controlled synthesis of micro- and nanocrystallites with specific surface structures is highly desired. Of note, previous research attention was mainly focused on the crystal growth in near equilibrium conditions. However, in supersaturated growth environments (nonequilibrium conditions), the corresponding crystal growth theories are still limited.

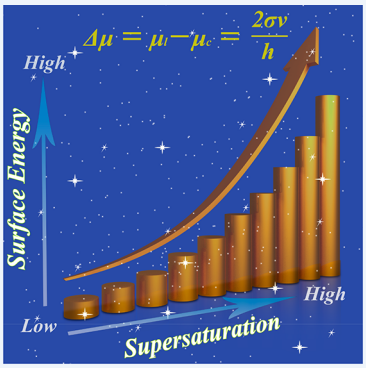

Recently, the supersaturation-controlled surface structure strategy, which is derived from thermodynamics and the Thomson−Gibbs equation, has opened up a new avenue for the control the surface structures of crystals. This strategy involves manipulating the supersaturation of growth units to control the surface structure of micro- and nanocrystallites, as the surface energy of exposed facets is correlated to the supersaturation of growth blocks. Based on the proposed theory, micro- and nanocrystallites with various surface structures, especially high-energy facets, have been successfully synthesized by our group and other researchers in past years. In order to draw lessons from previous studies, it is imperative to give a timely research account related to the supersaturation strategy and corresponding applications in controlling surface structures of different crystallites.

In this Account, we explore the supersaturation-controlled surface structure strategy to construct functional nanomaterials with desired architectures. First, we highlight the role of supersaturation of growth units from theoretical analysis after a short introduction of fundamental principles for crystal growth. Then, some detailed cases concerning evolution of surface structures are presented to highlight the key experimental factors involved in manipulating the supersaturation of growth units during synthetic processes. These factors include solvents, reaction rates, and additives in wet chemical routes as well as overpotential in electrochemical routes. In addition, we briefly discuss the role of supersaturation in growth kinetics with focus on explaining the formation of spherical micro- and nanocrystallites at extremely high supersaturation. Finally, a general summary of the supersaturation-dependent surface structure control and future prospects in this field are provided. It is expected that this Account will deepen the current understanding on fundamental principles behind the control of surface structures of micro- and nanocrystallites, which can help us to construct desirable nanomaterials and promote their practical applications.

1. INTRODUCTION

The rational design and controlled synthesis of micro- and nanocrystallites play a critical role in modern material chemistry because the distinctive and fascinating physicochemical properties of these materials can be precisely tuned by tailoring their crystal surface structures.[1−3] In past decades, considerable endeavors have been made in clarifying the relationship between the surface structures and physicochemical properties, especially in catalysis.[4,5] For example, in the synthesis of NH_3 over iron catalyst, the Fe(111) facets exhibit a kinetic rate that is several orders of magnitude higher than the Fe(100) facets.[6] When benzene hydrogenation was catalyzed on different Pt surfaces, a mixture of cyclohexene and cyclohexane was produced on Pt(111), while only cyclohexane formed on Pt(100).[7] However, these attractive results were mainly obtained from bulk single crystals. In fact, it would be practicable to bridge the gap between practical applications and fundamental surface science through rational control of the surface structures of micro- and nanocrystallites during crystal growth.[8−10]

During the past few decades, great efforts have been made in the controlled synthesis of micro- and nanocrystallites with specific surface structures by developing various synthetic approaches.[3,10,11] Typically, nanocrystals (NCs) with well-defined crystal facets can be prepared by carefully selecting surface-regulating agents that can thermodynamically reduce the surface energy via selective adsorption.[11] Many excellent review articles have summarized and discussed the roles of corresponding thermodynamic factors, such as capping

Received: July 10, 2018
Published: October 22, 2018

DOI: 10.1021/acs.accounts.8b00344
Acc. Chem. Res. 2018, 51, 2880−2887

effects.[9−13] However, due to complicated crystal growth environments and ambiguous roles of a variety of reaction reagents, the theoretical prediction and selection of surface-regulating agents are still difficult. Thus, the rational design and selective exposure of specific surface structures remain challenging.

In 2013, our group proposed a supersaturation-dependent growth strategy, derived from thermodynamics and the Thomson−Gibbs equation, and found that the surface energy of as-prepared micro- and nanocrystallites was correlated with the supersaturation of growth units.[14] Based on the proposed theory, several micro- and nanocrystallites with various surface structures, especially high-energy surfaces, ranging from noble metals, metal oxides, and ionic and molecular crystals to metal−organic frameworks (MOFs), have been successfully synthesized by our group and other researchers.[14−23] Noticeably, the supersaturation theory not only successfully explains a set of seemingly contradictory observations in the synthesis of micro- and nanocrystallites but also clarifies the relationship between apparent kinetic parameters (such as reduction rate) and the resulting surface structures. Thus, a comprehensive understanding of the role of supersaturation during the crystal growth is necessary, because it will shed light on the rational design and controlled synthesis of micro- and nanocrystallites with specific surface structures, thus greatly facilitating their performance in applications.

In this Account, we elaborate on the role of supersaturation in controlling the surface structures of micro- and nanocrystallites during crystal growth. After a short introduction of the fundamental principles for crystal growth, we focus on the role of supersaturation of growth units from theoretical analysis. Key experimental factors related to supersaturation are discussed and some detailed cases, including ionic crystals, molecular crystals, noble metals, metal oxides, and MOFs, are then presented. In addition, a short discussion about the role of supersaturation in growth kinetics is made with focus on the formation of spherical micro- and nanocrystallites at extremely high supersaturation. Finally, a general summary on supersaturation-dependent surface structure control and future prospects in this field are provided.

2. FUNDAMENTAL PRINCIPLES FOR CRYSTAL GROWTH UNDER SUPERSATURATED CONDITIONS

The crystallization in solution mainly involves generation of crystal units, nucleation and growth, which can be demonstrated by the LaMer curve (Figure 1a).[24] After a burst of nucleation, the crystal nuclei would grow into large crystals at nearly saturated conditions (nearly equilibrium conditions). And the shape of a crystallite can be predicted by the Wulff construction theorem:[25]

$$\frac{\sigma_i}{h_i} = \text{constant} \tag{1}$$

where σ and h are the specific surface energy and the distance from the crystallite's center to its surface, respectively.

From eq 1, one can see the high-energy crystal facets grow fast, their surface areas become small, and eventually crystals enclosed by low energy facets form (Figure 1b). Ideally, NCs with different surface structures might be prepared if one can tailor the surface energy through judiciously choosing different surface-regulating agents. For example, for wurtzite-type ZnO, hexagonal pyramidal ZnO with exposed high-energy {0001} and $\{10\bar{1}1\}$ polar planes can be obtained via oppositely charged species stabilizing these highly energetic planes.[26]

To clarify, previous research attention was mainly focused on the crystal growth in near equilibrium conditions. However, there are highly supersaturated growth environments (non-equilibrium conditions, purple zone in Figure 1a), where the supersaturation around the crystal nucleus is still high (but lower than the critical nucleation concentration (c_{min}^{nu})) with the proceeding of reaction, and the crystallites can also continually grow without forming new nuclei. Nevertheless, the corresponding crystal growth theories are still limited. A question arises as to how the crystallites also grow if the crystals grow under such conditions.

For crystal growth at constant pressure and temperature, the variation of Gibbs free energy (G) of the crystallization system could comply with eq 2:[14,25]

$$\Delta G = \mu_l dn_l + \mu_c dn_c + \sigma dS = 0 \tag{2}$$

where the subscripts l and c represent the solution and crystal phases, respectively. n and μ are the number of moles and chemical potentials of solutes (growth units), respectively. S and σ are the surface area and specific surface energy of crystallites, respectively.

From eq 2, it can be seen that when crystallization occurs, the excess energy (the difference between $\mu_l dn_l$ and $\mu_c dn_c$) would transfer to the surface energy of crystallites (σdS) due to the conservation of energy in an ideal crystal growth system. Furthermore, based on the eq 2, "Thomson−Gibbs"-like eq 3 can be readily deduced:

$$\Delta\mu = \mu_l - \mu_c = \frac{2\sigma v}{h} \tag{3}$$

where $\Delta\mu$ is the supersaturation and v is the volume of a single growth unit.

From eq 3, it is seen that the surface energy of crystallites (σ) increases with the increase of the supersaturation ($\Delta\mu$) at supersaturated growth conditions (nonequilibrium conditions). This means that the surface structures of crystals can be adjusted by tuning the supersaturation of growth units. The higher the supersaturation of growth units, the higher will be the surface energy of the NCs. And as μ_c is a nearly constant value at a given temperature, we may conclude from the eq 3 that the supersaturation of growth unit can be adjusted by its chemical potential.

For a growth unit in solution with a concentration of c, its chemical potential can be determined by eq 4

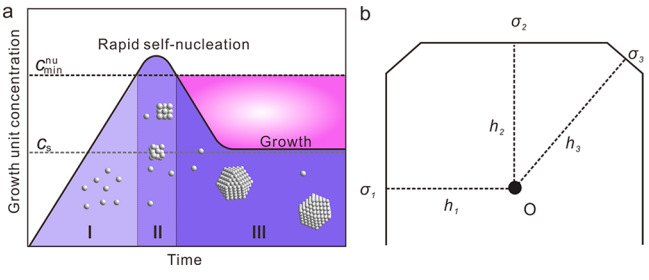

Figure 1. (a) LaMer curve illustrating three stages (generation of growth units (I), nucleation (II), and crystal growth (III)) of crystallization in a solution system. The light purple area abstractly represents the highly supersaturated growth condition. (b) Two-dimensional illustration of Wulff construction rule, where the order of specific surface energy (σ) of different facets follows: $\sigma_1 < \sigma_2 < \sigma_3$.

DOI: 10.1021/acs.accounts.8b00344
Acc. Chem. Res. 2018, 51, 2880−2887

$$\mu_1 = \mu_1^{\theta} + RT \ln c \quad (4)$$

where μ_1^{θ} stands for the standard chemical potential of the growth unit in solution, R is the gas constant, and T is the absolute temperature.

From eq 4, the chemical potential of a growth unit in solvent can be tuned by its μ_1^{θ} and c, which are correlated to the solubility and concentration of growth units in solution, respectively.[14]

3. FACTORS INFLUENCING SUPERSATURATION AND APPLICATION EXAMPLES

According to the above discussion, supersaturation-dependent growth should be a general route to control the exposed facets of various micro- and nanocrystallites. Next, based on the results of our group and others, we will classify and discuss the key factors for tuning supersaturation during practical processes and how they affect the surface structures of micro- and nanocrystallites.

3.1. Solvent

During the crystallization in solution, supersaturation is closely related to solvents. Evaporating solvent slowly is a classical method for crystal growth. However, in this process, the supersaturation of growth units at stage III in Figure 1 is usually very low, which results in crystal growth in near equilibrium conditions, thus forming crystals with low-energy facets. This is why naturally crystallized NaCl presents an almost perfect cubic shape bounded with stable {100} facets (Figure 2a). As discussed in section 2, the supersaturation of solute could be tuned by μ_1^{θ}. When the crystallization and dissolution reach the equilibrium point, $\mu_1 = \mu_c = \mu_1^{\theta} + RT \ln c$. Thus, μ_1^{θ} would be increased by lowering the solubility c (μ_c is a constant value), which can be achieved by varying the solvent.[14] As such, when a solution of NaCl in methanol (good solvent) was rapidly injected into a mixture of methanol and *n*-pentanol (poor solvent), continuous diffusion of *n*-pentanol into the methanol solvent would result in continuously high supersaturation of NaCl. Consequently, truncated rhombic dodecahedra (RD) bound with {100} and {110} facets, and RD with 12 high-energy {110} facets formed with gradually increasing the proportion of *n*-pentanol (Figure 2b,c).[14] Similarly, body-centered-cubic (bcc) molecular crystal 2,5,8,11-tetra-*tert*-butylperylene with different surface structures was also prepared via adjusting the supersaturation by changing the composition of solvents.[14]

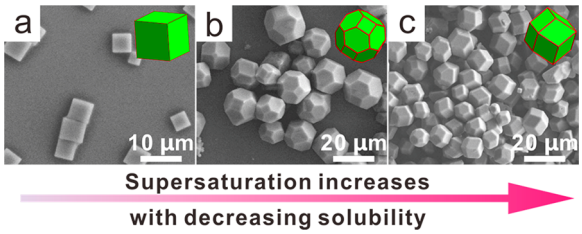

Figure 2. (a) Cubic NaCl microcrystals formed by slow evaporation of methanol. (b) Truncated RD and (c) perfect RD NaCl microcrystals obtained in the mixture of 2.00 mL of *n*-pentanol/1.25 mL of methanol and 2.00 mL of *n*-pentanol/1.00 mL of methanol, respectively. Reproduced with permission from ref 14. Copyright 2013 American Chemical Society.

A similar strategy to increase the supersaturation of growth blocks is also effective in the synthesis of crystallites via chemical reaction. For example, in the synthesis of α-Fe_2O_3 NCs by the hydrolysis of ferric acetylacetonate ($Fe(acac)_3$) via hydrothermal route, the surface structures can be controlled by varying the ratios of good solvent (ethanol) and poor solvent (water) (Figure 3).[18] Increasing the proportion of water in the solution greatly elevated the supersaturation of Fe^{3+}; accordingly, the products evolved from nanoplates with {001} facets to pseudocubes with higher energy {012} facets. Similar results were obtained in the synthesis of perovskite $NaTaO_3$.[27] The exposed surface transformed from low-energy {100} to high-energy {111} and {110} surfaces when the proportion of poor solvent in the growth solution was increased.

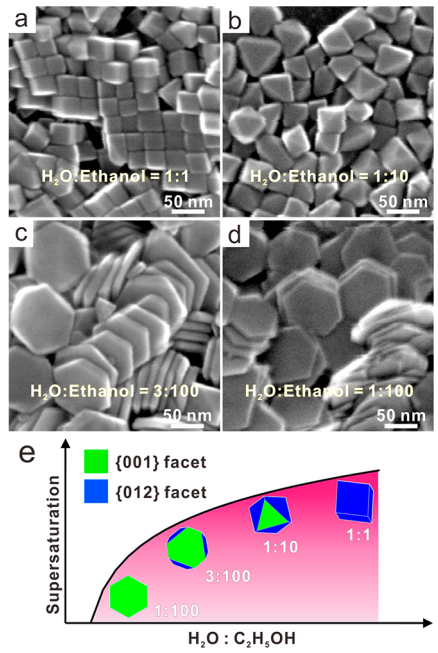

Figure 3. (a–d) Morphology evolution of α-Fe_2O_3 NCs in the presence of different H_2O/ethanol ratios. (e) Schematic of the supersaturation-dependent morphology evolution as a function of ratio of mixed solvents. Reproduced with permission from ref 18. Copyright 2014 American Chemical Society.

3.2. Reaction Rate

In most cases, micro- and nanocrystallites are prepared via chemical reactions. And the supersaturation of growth units can also be adjusted by changing the reaction rate. For example, during the preparation of noble-metal NCs, the process involves the following two steps:

Step 1

$$M^{n+}(\text{solution}) + ne^- \xrightarrow{r} M(\text{solution}, \mu_1)$$

Step 2

$$M(\text{solution}, \mu_1) \xrightarrow{\Delta\mu} M(\text{crystal}, \mu_c)$$

At step 1, the metal precursors (M^{n+}) are first reduced to the metallic atoms (M) at reduction rate r; then they grow on the crystallites driven by the supersaturation ($\Delta\mu$, step 2). Therefore, the chemical potential of metallic atoms in solution (μ_1) is relevant to the effective concentration of metallic atoms,

DOI: 10.1021/acs.accounts.8b00344
Acc. Chem. Res. 2018, 51, 2880–2887

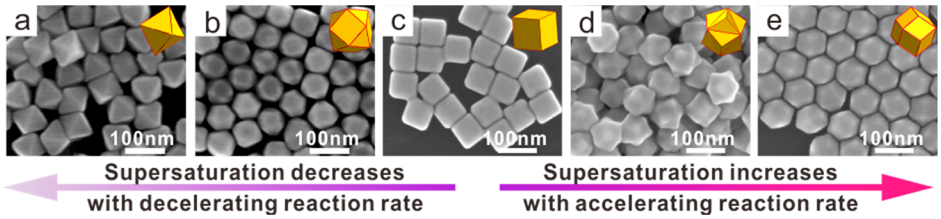

Figure 4. Morphology evolutions of Au NCs via tuning reaction rate: (c) cubic Au NCs transform to (b) cuboctahedral and (a) octahedral NCs with gradually decreasing injection rate of $HAuCl_4$; (c) cubic Au NCs transform to (d) TOH and (e) RD NCs with increasing amount of NaOH. Reproduced with permission from ref 14. Copyright 2013 American Chemical Society.

and thus the supersaturation of growth units will increase with the acceleration of *r*. Due to the high supersaturation of growth units, fast reduction rate would favor the formation of NCs with high surface energy.

Generally, the reaction rate is positively correlated to the concentration of metal precursors when the reductant is in large excess in the synthesis of noble metal NCs. For example, in the seed-mediated growth of Au NCs, the reaction rate was controlled by precisely varying the injection rate of precursors (total amount is the same) into a solution containing excess ascorbic acid (AA).[14] When the precursors were injected slower and slower, the morphology of Au NCs transformed from {100} faceted nanocubes to cuboctahedral NCs with {111} and {100} facets and finally octahedral NCs with low-energy {111} facets (Figure 4c,b,a). Clearly, if the injection rate is very fast, the available concentration of precursors is high, and thus the reduction rate is very fast, leading to the high supersaturation of growth blocks. When the injection rate slows, the supersaturation of growth units decreases accordingly, and thus low-energy facets are preferentially exposed (such as {111} facets).

In fact, reaction rate in the synthesis of noble metal NCs can be also adjusted in other ways. In our previous work, upon addition of NaOH into the growth solution to enhance the reducing strength of AA, Au NCs evolved from nanocubes with {100} facets to trioctahedra (TOH) with {331} facets and then to RD with {110} facets due to increasing reduction rate (i.e., higher and higher supersaturation) (Figure 4c,d,e).[14] Similar evolution phenomenon was observed upon elevation of the concentration of reductant relative to metal precursors. Xu's group demonstrated that convex hexoctahedral Pd@Au NCs with high-energy {431} facets were always produced at high molar ratio of AA to $HAuCl_4$, while {111}-faceted octahedral NCs formed at low molar ratio of AA to $HAuCl_4$.[28]

After understanding the relationship between reduction rate and the resulting surface structures, some results in the literature can also be well explained by the proposed supersaturation theory.[29−31] The fast reduction rate of noble metal precursors either by increasing the amount of reduction agent or elevating the pH of growth solution could always lead to the formation of NCs with high-energy facets due to high supersaturation of growth units. Examples can be found in the synthesis of Pd concave nanocubes,[29] Pd NCs with well-defined {100} (perfect cube) or high-energy {110} facets (perfect RD),[30] and concave Au−Pd bimetallic alloy NCs.[31]

Reaction temperature can also significantly change the reaction rates. According to the Van't Hoff rule, reaction rate will be accelerated 2−4 times when temperature is raised by about 10 °C. Hence, high supersaturation conditions can be readily achieved at high reaction temperature, thereby producing NCs with high-energy facets. For instance, octahedral Au NCs with low-energy {111} facets evolved to RD shape with high-energy {110} facets when the reaction temperature was raised from 20 to 30 °C.[32] Cubic Pd NCs with {100} facets became dominant at higher temperature (e.g., 80 °C), while cuboctahedral and truncated cubic Pd NCs formed at 30 or 40 °C.[30] Of note, we should be extremely cautious when discussing the temperature-dependent surface structure evolution of products, as reaction temperature can affect both the solubility of growth units and reaction rates. Therefore, we refrain from further discussion on this factor for now due to its complexity.

Apart from noble-metal NCs, it is also practicable to tailor the surface structures of other types of micro- and nanocrystallites by tuning the supersaturation via regulating reaction rates when the solute is generated by chemical reaction. In the synthesis of α-Fe_2O_3 NCs, the hydrolysis rate of precursor ($Fe(acac)_3$) was accelerated by directly increasing its concentration, thereby producing high-energy products, that is, {113} faceted hexagonal bipyramids.[18] Also, in the synthesis of $Cu_3(L)_2(DABCO)$, spindle-like morphology containing eight high-energy {103} facets could be prepared at high concentrations of precursors, as reported by Sun's group.[20] These results clearly indicate that a faster reaction rate would result in higher supersaturation, thus resulting in the formation of micro- and nanocrystallites with higher surface energy facets.

3.3. Effect of Additives

During the preparation of micro- and nanocrystallites via wet-chemical methods, in addition to the solvents and solutes (precursors), some additives, including surfactants and inorganic salts, are deliberately added in order to change the crystal growth behavior. In many cases, these additives act as shape regulators via the "capping" effect, and their roles have been well-documented in many excellent review articles.[9−13] However, in some cases, contradictory conclusions are drawn when only the "capping" effect is taken into consideration. For instance, it was suggested that cetyltrimethylammonium bromide (CTAB) could selectively stabilize the {100} facets of Au NCs, resulting in the formation of Au nanocubes exclusively.[32,33] Nevertheless, Au NCs with various surface structures have been prepared with CTAB in many studies.[34−36] This indicates that other roles of additives should be considered beyond the well-known capping effect.

In fact, additives may act in different ways to affect the crystallization. They may interact with precursors and accordingly alter the reduction potential of precursors or the available amount of precursors. Consequently, the supersaturation of growth units and the resulting surface structures of products may be tuned. Take the synthesis of Pd NCs, for example. Tetrahexahedral Pd NCs with high-energy {730} facets were prepared by directly reducing H_2PdCl_4 with AA without using any surfactants.[14] In contrast, cubic Pd

DOI: 10.1021/acs.accounts.8b00344
Acc. Chem. Res. 2018, 51, 2880−2887

nanocubes with stable {100} facets formed when cetyltrimethylammonium chloride (CTAC) was added to the growth solution. Clearly, this morphology evolution cannot be fully explained by the specific adsorption of either CTA^+ ions or Cl^- ions on Pd. However, this result is easily understood from the aspect of supersaturation. In fact, newly added CTAC would suppress the reduction rate of precursors due to their coordination with Pd^{2+} ions, which would lead to a state of low supersaturation. Thus, the product with low-energy surface is naturally favored. This result hints that noble metal NCs of different surface structures could be achieved by precisely tuning the coordination of additives with metal ions. In another case, as the ratio of CTAB to CTAC increased, the reaction rate decreased accordingly due to the stronger coordination ability of Br^- with Pd^{2+} ions than Cl^-. Consequently, the Pd NCs evolved from concave nanocubes with high-energy {730} facets to slightly concave nanocubes with relatively low-energy facets (Figure 5).[37]

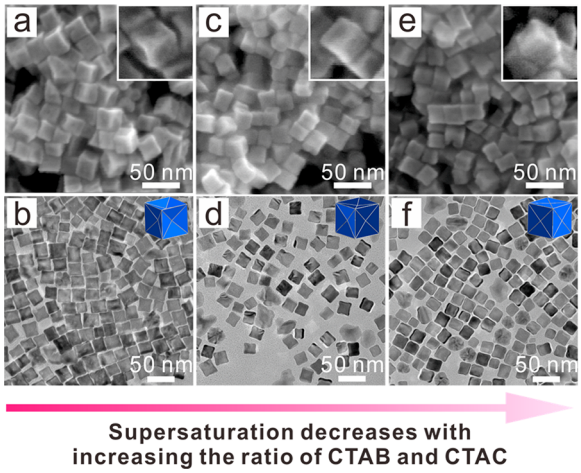

Figure 5. Morphology evolution of Pd NCs upon adjusting surfactant ratios: SEM (top) and corresponding TEM images (bottom) of concave cubic Pd NCs with flatter surface along with increasing the ratio of CTAB/CTAC (a, b) 4:1, (c, d) 1:1, (e, f) 1:4. Reproduced with permission from ref 37. Copyright 2011 John Wiley and Sons.

Similarly, in the synthesis of MOFs, some additive may affect the supersaturation of growth units by interacting with the reactant. For example, Sun's group found that the supersaturation of growth units for HKUST-1 was suppressed by adding inorganic salt ions like Na^+ and K^+ into the growth solution, because the added salt ions reduced the available concentration of negative ligands through electrostatic interactions.[22] As a result, cubic HKUST-1 with {100} facets transformed into the octahedra with low-energy {111} facets.

In addition to directly reacting with precursors, some additives may indirectly change the concentration of precursors (corresponding to supersaturation), which in turn would result in the formation of products with various surface structures. For example, Lin's group successfully prepared two-dimensional layered MOFs with high surface energy by adding water to the reaction mixture, which was attributed to the high concentration of metal clusters produced by the partial hydrolysis of Hf^{4+} in water.[21] Also, Sun's group reported the evolution of bcc MOF-14 from low-energy {110} faceted RD to high-energy {100} faceted cube by adding base in the growth solution (Figure 6).[16] In this case, addition of base effectively accelerated the deprotonation rate of ligand and led to the fast coordination rate with Cu ions, thus yielding high supersaturation of growth units. The above examples demonstrate that one can control the morphology of crystals by intentionally tuning the supersaturation of growth units with additives.

3.4. Overpotential in Electrochemical Synthesis

In the above sections, we mainly discussed the role of supersaturation in tailoring the surface structures of micro- and nanocrystallites through wet-chemical routes. In fact, the concept of supersaturation-controlled surface structure is also valid for the synthesis of nanocrystallites via electrochemical routes. In electrochemical synthesis, the supersaturation of growth units ($\Delta\mu$) is positively correlated to the overpotential (η), and this relationship can be expressed as eq 5:[25,38]

$$\Delta\mu = ze\eta \tag{5}$$

where z and e denote the valence of the neutralizing ions and the elementary electric charge, respectively. Clearly, the supersaturation increases with the increase of overpotential. In the controlled synthesis of bcc Fe NCs via electrochemical route, Sun et al. successfully demonstrated that the proportion of high-energy {100} facets on the as-deposited Fe NCs can be finely increased with increasing the overpotentials (Figure 7).[15] Accordingly, Fe NCs with RD or tetragonal bipyramidal shape that are all bounded by low-energy {110} facets finally evolved to cubic NCs with high-energy {100} facets.

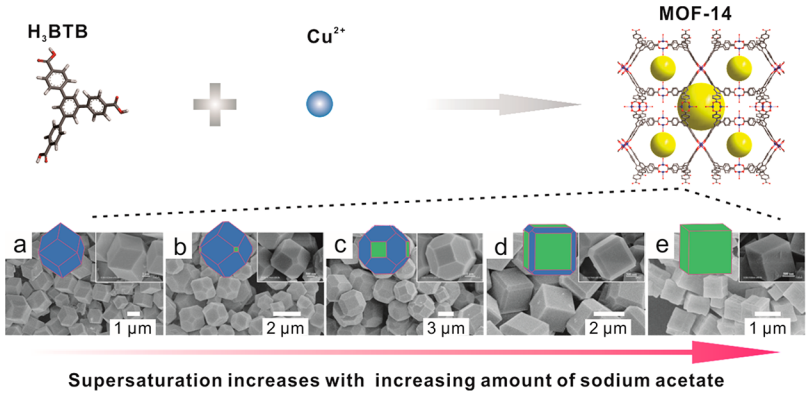

Figure 6. Morphology evolution of MOF-14 upon addition of (a) 0, (b) 1, (c) 2, (d) 3, and (e) 4 equiv of sodium acetate (with respect to H_3BTB). Reproduced with permission from ref 16. Copyright 2014 John Wiley and Sons.

DOI: 10.1021/acs.accounts.8b00344
Acc. Chem. Res. 2018, 51, 2880−2887

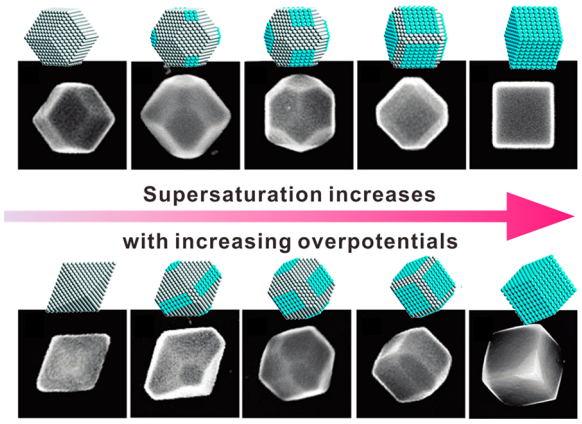

Figure 7. Shape evolution of two series of Fe NCs from low-energy (110) facets to high-energy (100) facets with increasing the overpotential. Gray color, (110) facet; cyan color, (100) facet. Reproduced with permission from ref 15. Copyright 2009 American Chemical Society.

4. THE ROLE OF SUPERSATURATION IN GROWTH KINETICS IN THE FORMATION OF SPHERE-LIKE NANOPARTICLES

During the crystal growth, the thermodynamics governs the growth tendency, while the kinetics deals with the energy barriers of growth units on different specific crystal facets and the specific growth pathways.[12] As the driving force for crystallization, supersaturation also plays a part in manipulating the growth kinetics. A typical example is the formation of sphere-like nanoparticles at very high supersaturated conditions.

In the synthesis of $NaTaO_3$ microcrystallites, quasi-sphere single-crystal $NaTaO_3$ was obtained when the supersaturation was greatly increased by using different solvents and additives (Figure 8).[27] However, the formation of sphere-like crystallites is difficult to explain by the classical Wulff construction rule, which uncovers the shapes of crystals under thermodynamic equilibrium conditions. If crystal growth kinetics, specifically

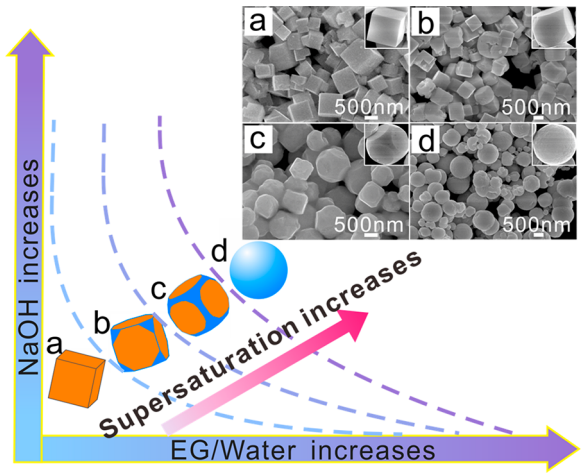

Figure 8. Morphology evolution of $NaTaO_3$ crystallites from (a) cubic particles to (b) corner-truncated cubes, (c) corner and edge truncated cubes, and (d) quasi-spherical particles with increasing the volume ratios of ethylene glycol to water. Reproduced with permission from ref 27. Copyright 2015 Science China Press and Springer-Verlag Berlin Heidelberg.

the formation work of two-dimension crystal nuclei (activation barrier) on different specific crystal facets (W_{hkl}), is taken into consideration, the formation of quasi-spherical crystallites at extremely high supersaturation can be adequately explained.[25,27]

For ideal crystal growth on a single crystal seed, the crystal growth rate normal to the crystal facet (ν_{hkl}) is proportional to W_{hkl}, as shown in eq 6:[25]

$$\nu_{hkl} \propto \exp\left(-\frac{W_{hkl}}{kT}\right) \tag{6}$$

where hkl represents the indices of the crystal facet, k is the Boltzman's constant, and T is the absolute temperature.

And the formation work W_{hkl} can be expressed by eq 7, regardless of the type of crystal lattice:[25]

$$W_{hkl} = \frac{B_{hkl}}{\frac{\Delta\mu}{mN} - A_{hkl}} \tag{7}$$

where m and N are the atom number and Avogadro's constant, respectively. A_{hkl} and B_{hkl} are constants depending on the bond-breaking work in the crystal lattice.

From eqs 6 and 7, it can be seen that the supersaturation of the growth units can greatly influence the W_{hkl}, and in turn the crystal growth rate normal to the specific crystal facet could be tuned. When the supersaturation is low (near the equilibrium condition), W_{hkl} is determined by the A_{hkl} and B_{hkl}, which are related to the surface energy of crystal facets. It can be deduced that the crystal facets with low surface energy prefer to be exposed, which is in accordance to the shapes predicted by the Wulff construction rule.[38,39] On the other hand, when the supersaturation is extremely high, W_{hkl} could tend to be zero. Therefore, various crystal facets would have similar crystal growth rates, which results in the formation of quasi-spherical or spherical crystals. This conclusion is consistent with the *in situ* TEM observation of the cubic Pt NCs growth in a liquid cell, which clearly demonstrated that the Pt NCs grew along different directions (i.e., ⟨100⟩, ⟨111⟩, and ⟨110⟩ axes) at a similar rate during the initial growth stage.[40] Actually, during crystal growth, the supersaturation of growth units decreases along with the reaction time. Therefore, the products with high-energy facets may form during the early growth stage. For example, high-energy {113} faceted hexagonal bipyramidal α-Fe_2O_3 NCs were found at the beginning of the reaction, while pseudocubic NCs with low-energy {012} facets were produced when the reaction time was prolonged.[18] In the synthesis of MOF-5, concave octahedra with high surface energy were produced during the initial growth stage.[19]

In the above discussion, we focused on nonequilibrium crystal growth under highly supersaturated environments. In addition, there exists another nonequilibrium growth situation, where the concentration of growth units near the crystal nucleus is depleted.[41] Under such growth conditions, fractal or dendritic architectures usually form. This growth behavior can be explained by diffusion-limited aggregation (DLA) and nucleation-limited aggregation (NLA) models.[42,43] Due to the limitation of space, deeper discussion about this issue is not presented in this Account.

5. CONCLUDING REMARKS

Over the past decades, numerous studies have demonstrated the critical role of surface structures of micro- and nanocrystallites in improving specific physicochemical properties,

DOI: 10.1021/acs.accounts.8b00344
Acc. Chem. Res. 2018, 51, 2880−2887

especially for heterogeneous catalysis. The famous Gibbs–Wulff theorem determines the polyhedral shape of crystals grown in thermodynamic equilibrium conditions, and the DLA or NLA models can suitably describe the formation of fractal or dendritic structures when the concentration of growth units near the crystal nucleus is depleted (far from thermodynamic equilibrium). The proposed supersaturation strategy enhances the understanding of crystal growth at high supersaturated conditions (nonequilibrium conditions) and has been proven to be an effective approach for the designed synthesis of micro- and nanocrystallites with various surface structures. Importantly, several contradictory conclusions could be answered from the perspective of supersaturation, and moreover, the relationship between the apparent kinetic parameters (e.g., reaction rate and time) and the final surface structures could also be clarified.

To date, it is still difficult to address how to maintain high supersaturation of growth units for a specific crystal growth system. The specific approach varies depending on the system. For example, during the synthesis of noble metal NCs, the straightforward approach to increase the supersaturation of growth units is to accelerate the reduction rate. For the synthesis of MOFs, it is advisable to increase the supersaturation of growth units through increasing the concentration of organic ligands or metal ions or clusters. It should be noted that the supersaturation cannot be infinitely increased as it may lead to the occurrence of secondary nucleation when the supersaturation reaches the critical value for nucleation.

During the crystal growth, the growth kinetics plays a key role in the formation of various kinds of surface structures. Although progress has been made in explaining and controlling the growth behaviors of crystals by considering kinetics, it is still particularly complicated to clarify the specific roles of numerous kinetic parameters (including reaction temperature, diffusion, and mass transport) in different reaction conditions. In future, more attention needs to be paid to investigating this aspect.

AUTHOR INFORMATION

Corresponding Authors

*E-mail: qkuang@xmu.edu.cn (Q.K.).
*E-mail: zxxie@xmu.edu.cn (Z.X.X.).

ORCID

Jiawei Zhang: 0000-0001-9635-154X
Qin Kuang: 0000-0002-4111-291X
Zhaoxiong Xie: 0000-0002-4225-6536

Notes

The authors declare no competing financial interest.

Biographies

Jiawei Zhang gained his Ph.D. degree from Xiamen University under the supervision of Prof. Zhaoxiong Xie in 2015. Currently, he is a postodoctoral fellow in Prof. Xie's group. His research focuses on the controlled synthesis of noble metal nanocrystals and their applications in catalysis and fuel cells.

Huiqi Li is currently pursuing her Ph.D. degree at Xiamen University under the supervision of Prof. Zhaoxiong Xie. Her interest focuses on wet chemical synthesis of noble metal-based nanocrystals with excavated structures and their applications in catalysis.

Qin Kuang received his B.S. (2001) in Chemistry and Ph.D. (2008) in Inorganic Chemistry from Xiamen University, China. He is currently a Professor of Chemistry at Xiamen University. His current research is focused on surface/interface engineering of inorganic functional nanomaterials and their applications in the energy conversion and environmental fields.

Zhaoxiong Xie received his B.S. (1987) in Chemistry and his M.S. (1990) and Ph.D. (1995) in Physical Chemistry from Xiamen University, China. Since 2002, he has held the position of Professor of Chemistry at Xiamen University. His current research is focused on the surface/interface chemistry of functional nanocrystals and self-assemblies of molecules via weak interactions on solid surfaces.

ACKNOWLEDGMENTS

This work was supported by the National Basic Research Program of China (No. 2015CB932301), the National Key Research and Development Program of China (2017YFA0206500 and 2017YFA0206801), the National Natural Science Foundation of China (No. 21333008, 21603178, 21671163. and 21773190), and China Postdoctoral Science Foundation (2016M602066, 2017T100468). We are grateful to our collaborators and other workers, as cited, for their invaluable contributions to this research field.

REFERENCES

(1) Burda, C.; Chen, X.; Narayanan, R.; El-Sayed, M. A. Chemistry and Properties of Nanocrystals of Different Shapes. *Chem. Rev.* **2005**, *105*, 1025−1102.
(2) Wiley, B.; Sun, Y.; Xia, Y. Synthesis of Silver Nanostructures with Controlled Shapes and Properties. *Acc. Chem. Res.* **2007**, *40*, 1067−1076.
(3) Niu, W.; Xu, G. Crystallographic Control of Noble Metal Nanocrystals. *Nano Today* **2011**, *6*, 265−285.
(4) Somorjai, G. A. Modern Surface Science and Surface Technologies: An Introduction. *Chem. Rev.* **1996**, *96*, 1223−1235.
(5) Ye, R.; Hurlburt, T. J.; Sabyrov, K.; Alayoglu, S.; Somorjai, G. A. Molecular Catalysis Science: Perspective on Unifying The Fields of Catalysis. *Proc. Natl. Acad. Sci. U. S. A.* **2016**, *113*, 5159−5166.
(6) Strongin, D. R.; Carrazza, J.; Bare, S. R.; Somorjai, G. A. The Importance of C7 Sites and Surface Roughness in The Ammonia Synthesis Reaction over Iron. *J. Catal.* **1987**, *103*, 213−215.
(7) Bratlie, K. M.; Kliewer, C. J.; Somorjai, G. A. Structure Effects of Benzene Hydrogenation Studied with Sum Frequency Generation Vibrational Spectroscopy and Kinetics on Pt(111) and Pt(100) Single-crystal Surfaces. *J. Phys. Chem. B* **2006**, *110*, 17925−17930.
(8) Jiang, Z.; Kuang, Q.; Xie, Z.; Zheng, L. Syntheses and Properties of Micro/Nanostructured Crystallites with High-energy Surfaces. *Adv. Funct. Mater.* **2010**, *20*, 3634−3645.
(9) Chen, Q.; Jia, Y.; Xie, S.; Xie, Z. Well-faceted Noble-metal Nanocrystals with Nonconvex Polyhedral Shapes. *Chem. Soc. Rev.* **2016**, *45*, 3207−3220.
(10) Zhang, J.; Kuang, Q.; Jiang, Y.; Xie, Z. Engineering High-energy Surfaces of Noble Metal Nanocrystals with Enhanced Catalytic Performances. *Nano Today* **2016**, *11*, 661−677.
(11) Xia, Y.; Xiong, Y.; Lim, B.; Skrabalak, S. E. Shape-controlled Synthesis of Metal Nanocrystals: Simple Chemistry Meets Complex Physics? *Angew. Chem., Int. Ed.* **2009**, *48*, 60−103.
(12) Wang, Y.; He, J.; Liu, C.; Chong, W.; Chen, H. Thermodynamics versus Kinetics in Nanosynthesis. *Angew. Chem., Int. Ed.* **2015**, *54*, 2022−2051.
(13) Chen, M.; Wu, B.; Yang, J.; Zheng, N. Small Adsorbate-assisted Shape Control of Pd and Pt Nanocrystals. *Adv. Mater.* **2012**, *24*, 862−879.
(14) Lin, H.; Lei, Z.; Jiang, Z.; Hou, C.; Liu, D.; Xu, M.; Tian, Z.; Xie, Z. Supersaturation-dependent Surface Structure Evolution: from Ionic, Molecular to Metallic Micro/Nanocrystals. *J. Am. Chem. Soc.* **2013**, *135*, 9311−9314.

DOI: 10.1021/acs.accounts.8b00344
Acc. Chem. Res. 2018, 51, 2880−2887

(15) Chen, Y.; Chen, S.; Zhou, Z.; Tian, N.; Jiang, Y.; Sun, S.; Ding, Y.; Wang, Z. Tuning The Shape and Catalytic Activity of Fe Nanocrystals from Rhombic Dodecahedra and Tetragonal Bipyramids to Cubes by Electrochemistry. *J. Am. Chem. Soc.* **2009**, *131*, 10860−10862.
(16) Liu, Q.; Yang, J.; Jin, L.; Sun, W. Controlled Synthesis of Porous Coordination-Polymer Microcrystals with Definite Morphologies and Sizes under Mild Conditions. *Chem. - Eur. J.* **2014**, *20*, 14783−14789.
(17) Meng, M.; Wu, X.; Zhu, X.; Yang, L.; Gan, Z.; Zhu, X.; Liu, L.; Chu, P. Cubic In_2O_3 Microparticles for Efficient Photoelectrochemical Oxygen Evolution. *J. Phys. Chem. Lett.* **2014**, *5*, 4298−4304.
(18) Ouyang, J.; Pei, J.; Kuang, Q.; Xie, Z.; Zheng, L. Supersaturation-controlled Shape Evolution of α-Fe_2O_3 Nanocrystals and Their Facet-dependent Catalytic and Sensing Properties. *ACS Appl. Mater. Interfaces* **2014**, *6*, 12505−12514.
(19) Zhang, Z.; Chen, Y.; Xu, X.; Zhang, J.; Xiang, G.; He, W.; Wang, X. Well-defined Metal-organic Framework Hollow Nanocages. *Angew. Chem., Int. Ed.* **2014**, *53*, 429−433.
(20) Qi, Z.; Yang, J.; Kang, Y.; Sun, W. Morphology Evolution and Gas Adsorption of Porous Metal-organic Framework Microcrystals. *Dalton Trans.* **2015**, *44*, 16888−16893.
(21) Cao, L.; Lin, Z.; Peng, F.; Wang, W.; Huang, R.; Wang, C.; Yan, J.; Liang, J.; Zhang, Z.; Zhang, T.; Long, L.; Sun, J.; Lin, W. Self-supporting Metal-Organic Layers as Single-site Solid Catalysts. *Angew. Chem., Int. Ed.* **2016**, *55*, 4962−4966.
(22) Liu, Q.; Yang, J.; Jin, L.; Sun, W. Metal Ion Induced Porous HKUST-1 Nano/Microcrystals with Controllable Morphology and Size. *CrystEngComm* **2016**, *18*, 4127−4132.
(23) Ng, C. H. B.; Fan, W. Crystal Origami: Preparation of β-Ag_2MoO_4 Concave and Convex Crystals with High-index Facets. *ChemNanoMat* **2017**, *3*, 178−182.
(24) LaMer, V.; Dinegar, R. Theory, Production and Mechanism of Formation of Monodispersed Hydrosols. *J. Am. Chem. Soc.* **1950**, *72*, 4847−4854.
(25) Markov, I. *Crystal Growth for Beginners: Fundamentals of Nucleation, Crystal Growth, and Epitaxy*; World Scientific: Singapore; River Edge, N. J., 2003.
(26) Zhou, X.; Xie, Z.; Jiang, Z.; Kuang, Q.; Zhang, S.; Xu, T.; Huang, R.; Zheng, L. Formation of ZnO Hexagonal Micro-pyramids: A Successful Control of The Exposed Polar Surfaces with The Assistance of Anionic Liquid. *Chem. Commun.* **2005**, 5572−5574.
(27) Chen, W.; Kuang, Q.; Xie, Z. Morphology Evolution of $NaTaO_3$ Submicrometer Single-crystals: from Cubes to Quasi-spheres. *Sci. China Mater.* **2015**, *58*, 281−288.
(28) Zhang, L.; Niu, W.; Gao, W.; Qi, L.; Lai, J.; Zhao, J.; Xu, G. Synthesis of Convex Hexoctahedral Palladium@Gold Core-shell Nanocrystals with {431} High-index Facets with Remarkable Electrochemiluminescence Activities. *ACS Nano* **2014**, *8*, 5953−5958.
(29) Niu, W.; Zhang, W.; Firdoz, S.; Lu, X. Controlled Synthesis of Palladium Concave Nanocubes with Sub-10-nanometer Edges and Corners for Tunable Plasmonic Property. *Chem. Mater.* **2014**, *26*, 2180−2186.
(30) Niu, W.; Zhang, L.; Xu, G. Shape-controlled Synthesis of Single-crystalline Palladium Nanocrystals. *ACS Nano* **2010**, *4*, 1987−1996.
(31) DeSantis, C.; Sue, A.; Bower, M.; Skrabalak, S. Seed-mediated Co-reduction: A Versatile Route to Architecturally Controlled Bimetallic Nanostructures. *ACS Nano* **2012**, *6*, 2617−2628.
(32) Niu, W.; Zheng, S.; Wang, D.; Liu, X.; Li, H.; Han, S.; Chen, J.; Tang, Z.; Xu, G. Selective Synthesis of Single-crystalline Rhombic Dodecahedral, Octahedral, and Cubic Gold Nanocrystals. *J. Am. Chem. Soc.* **2009**, *131*, 697−703.
(33) Sau, T. K.; Murphy, C. J. Room Temperature, High-yield Synthesis of Multiple Shapes of Gold Nanoparticles in Aqueous Solution. *J. Am. Chem. Soc.* **2004**, *126*, 8648−8649.
(34) Wu, H.; Kuo, C.; Huang, M. H. Seed-mediated Synthesis of Gold Nanocrystals with Systematic Shape Evolution from Cubic to Trisoctahedral and Rhombic Dodecahedral Structures. *Langmuir* **2010**, *26*, 12307−12313.
(35) Eguchi, M.; Mitsui, D.; Wu, H. L.; Sato, R.; Teranishi, T. Simple Reductant Concentration-dependent Shape Control of Polyhedral Gold Nanoparticles and Their Plasmonic Properties. *Langmuir* **2012**, *28*, 9021−9026.
(36) Langille, M. R.; Personick, M. L.; Zhang, J.; Mirkin, C. A. Defining Rules for The Shape Evolution of Gold Nanoparticles. *J. Am. Chem. Soc.* **2012**, *134*, 14542−14554.
(37) Zhang, J.; Zhang, L.; Xie, S.; Kuang, Q.; Han, X.; Xie, Z.; Zheng, L. Synthesis of Concave Palladium Nanocubes with High-index Surfaces and High Electrocatalytic Activities. *Chem. - Eur. J.* **2011**, *17*, 9915−9919.
(38) Pangarov, N. A. On The Crystal Orientation of Electrodeposited Metals. *Electrochim. Acta* **1964**, *9*, 721−726.
(39) Pangarov, N. A. The Crystal Orientation of Electrodeposited Metals. *Electrochim. Acta* **1962**, *7*, 139−146.
(40) Liao, H.; Zherebetskyy, D.; Xin, H.; Czarnik, C.; Ercius, P.; Elmlund, H.; Pan, M.; Wang, L.; Zheng, H. Facet Development during Platinum Nanocube Growth. *Science* **2014**, *345*, 916−919.
(41) Zhang, J.; Chen, M.; Chen, J.; Li, H.; Wang, S.; Kuang, Q.; Cao, Z.; Xie, Z. Synthesis of Single-crystal Hyperbranched Rhodium Nanoplates with Remarkable Catalytic Properties. *Sci. China Mater.* **2017**, *60*, 685−696.
(42) Ming, N.; Wang, M.; Peng, R. Nucleation-limited Aggregation in Fractal Growth. *Phys. Rev. E: Stat. Phys., Plasmas, Fluids, Relat. Interdiscip. Top.* **1993**, *48*, 621−624.
(43) Witten, T. A.; Sander, L. M. Diffusion-limited Aggregation, A Kinetic Critical Phenomenon. *Phys. Rev. Lett.* **1981**, *47*, 1400−1403.

DOI: 10.1021/acs.accounts.8b00344
Acc. Chem. Res. 2018, 51, 2880−2887